EDGE ARTICLE

Check for updates

Cs₃VO(O₂)₂CO₃: an exceptionally thermostable carbonatoperoxovanadate with an extremely large second-harmonic generation response†

Guohong Zou, [ID] *[a] Zhien Lin, [ID] [a] Hongmei Zeng,[a] Hongil Jo, [ID] [b] Seong-Ji Lim,[c] Tae-Soo You [ID] [c] and Kang Min Ok [ID] *[b]

A novel nonlinear optical (NLO) carbonatoperoxovanadate, Cs₃VO(O₂)₂CO₃, with an exceptionally high thermostability was successfully synthesized by introducing highly polarizable Cs⁺ cations and inorganic polydentate carbonate anions into asymmetric peroxovanadates. The structure of Cs₃VO(O₂)₂CO₃ is composed of distorted [VO(O₂)₂CO₃]³⁻ units and charge balancing Cs⁺ cations. The title compound exhibits the largest NLO intensity ever found in the current carbonate NLO materials, *i.e.*, 23.0 times that of KH₂PO₄ (KDP). The remarkably strong second-harmonic generation (SHG) response originates from the synergistic effect of the exceedingly polarizable Cs⁺ cations, distortive polyhedra of the V⁵⁺ cation, delocalized π orbitals in CO₃ groups, and distorted localized π orbitals in O₂ groups. First-principles calculations indicated that introducing the polarizable cations into peroxovanadates not only induces the enhancement of the SHG response but also improves the thermal stability of the framework.

The development and availability of nonlinear optical (NLO) crystals,[1–15] key materials for solid state lasers to produce continuously tunable coherent light by means of cascaded frequency conversion, have attracted extensive interest owing to their various adaptable applications. A superb NLO material[16–19] should meet the following criteria: (1) larger SHG coefficient (d_{ij}) than d_{36} of KDP, (2) wide transparency range, (3) suitable birefringence to achieve the phase-matching condition, (4) large laser damage threshold, (5) good physicochemical and mechanical properties, and (6) easy growth of high quality large crystals. After decades of efforts by chemists and materials scientists to promote the development of novel NLO materials, a number of excellent NLO materials covering a broad wavelength range from ultraviolet (UV) and visible to mid-infrared (IR) have been discovered. Several widely utilized representative NLO materials include KH₂PO₄ (KDP),[20] KTiOPO₄ (KTP),[21] LiNbO₃,[22] LiB₃O₅ (LBO),[23] β-BaB₂O₄ (β-BBO),[24] and AgGaS₂ (AGS).[25] However, each of the NLO materials has some specific drawbacks such as unbefitting birefringence and toxicity of raw materials.[26,27] Thus, the demand for superior performing

flawless NLO materials that can satisfy the increasing needs of the scientific and technological development still remains high. Since the SHG coefficient is a crucial factor that directly affects the efficiency of the laser, a systematic synthesis of novel NLO materials with strong SHG response is essential.

Employing noncentrosymmetric (NCS) chromophores during the initial syntheses as building blocks has been suggested to be a very effective strategy toward new NLO materials.[28–30] Moreover, introducing more than two NCS chromophores into a compound could further induce a strong SHG response through the cooperative effect of the asymmetric chromophores. A few NCS chromophores include polar displacement of a d^{10} cation center, distorted polyhedra with d^0 transition metal cations and/or stereochemically active lone pairs (SCALPs) resulting from the second-order Jahn–Teller (SOJT) effect, and delocalized π-orbital anionic groups.[31–40] Recently, Ye and coworkers have proven that O₂²⁻ anion groups could also make huge contributions to the NLO effect as the symmetric distribution of localized π-orbital electrons is broken when the O₂²⁻ groups are coordinated to a d^0 cation, V⁵⁺.[41] We have recently demonstrated that employing inorganic polydentate carbonato groups in NCS peroxovanadates induced a sharp enhancement of the SHG response.[42] Therefore, carbonatoperoxovanadates can be used as latent capacity NLO materials for practical applications. Thus far, however, the significant influence of charge balancing cations on the overall SHG intensity has not been well recognized compared to that of the anionic group theory when designing new NLO materials.[43] Recently, a few novel NLO materials revealing large SHG

[a]College of Chemistry, Sichuan University, Chengdu 610064, P. R. China. E-mail: zough@scu.edu.cn

[b]Department of Chemistry, Chung-Ang University, Seoul 06974, Republic of Korea. E-mail: kmok@cau.ac.kr

[c]Department of Chemistry, Chungbuk National University, Cheongju, Chungbuk 28644, Republic of Korea

† Electronic supplementary information (ESI) available. CCDC 1851047. For ESI and crystallographic data in CIF or other electronic format see DOI: 10.1039/c8sc03672a

responses with highly polarizable cations such as Li_2CsPO_4 [44–46] and $Ba_4B_{11}O_{20}F$ [47] have been reported, where the increased polarization of cations with larger radii was beneficial to strong SHG intensity. Guided by these ideas, we have introduced a large alkali metal cation, Cs^+, into a carbonatoperoxovanadate and successfully synthesized a novel highly thermostable NLO material, $Cs_3VO(O_2)_2CO_3$, in high yield. Surprisingly, $Cs_3VO(O_2)_2CO_3$ exhibits an SHG intensity of *ca.* 23.0 times that of KDP, the strongest SHG response ever found in NLO carbonates. In this manuscript, the origin of the extremely strong SHG intensity and the high stability of $Cs_3VO(O_2)_2CO_3$ is elucidated by comparison with other stoichiometrically equivalent alkali metal carbonatoperoxovanadates.

Yellow plate-like crystals of $Cs_3VO(O_2)_2CO_3$ were synthesized *via* a modified solution-evaporation method (Fig. S1†). The powder X-ray diffraction (PXRD) pattern of the ground crystals of $Cs_3VO(O_2)_2CO_3$ confirms the phase purity (Fig. S2†). $Cs_3VO(O_2)_2CO_3$, isostructural to $A_3VO(O_2)_2CO_3$ (A = K and Rb), [41,42] crystallizes in the polar NCS space group of *Cm* (no. 8). The structure of $Cs_3VO(O_2)_2CO_3$ is composed of isolated $[VO(O_2)_2CO_3]^{3-}$ complex anions and Cs^+ ions as charge balancing cations (Fig. 1). V^{5+} cations reveal a seven-coordinate $VO_3(O_2)_2$ distorted pentagonal bipyramid (pbp) geometry with oxygen atoms (O3 and O5) in a carbonato group, a double-bonded oxygen atom (O1) at the axial position, and two sets of oxygen atoms (O2 and O6) in peroxo groups. The equatorial plane, defined by four oxygen atoms (two O2 and two O6) from two peroxide anions $(O_2)^{2-}$ and the carbonato oxygen atom (O3), is perpendicular to a crystallographic mirror plane that is composed of a $(CO_3)^{2-}$ group, a V^{5+} cation, and the double-

bonded oxygen atom (O1). The bonds between V^{5+} and oxide ligands in the apical position are significantly weaker than those between V^{5+} and equatorial O ligands due to the trans influence [2.311(11) Å *vs.* 1.860(8)–2.044(11) Å]. The observed $V=O_{apical}$ bond distance of 1.624(11) Å is similar to the average value of 1.609 Å, found in peroxovanadates. The C–O bond lengths in the $(CO_3)^{2-}$ planar triangular group are in the range of 1.258(18)–1.345(18) Å. The different C–O bond distances observed in the $(CO_3)^{2-}$ groups are attributed to the presence of further bonds of oxygen with other atoms. The short C–O bond length between C1 and the terminal oxygen O4 [1.258(18) Å] indicates a significant double-bond character. The stronger the C–O bonds [C–O5 (1.27(2) Å) *vs.* the C–O3 bond (1.345(18) Å)], the weaker the corresponding V–O bonds [V–O5 (2.311(11) Å) *vs.* V–O3 (2.044(11) Å)]. The $VO_3(O_2)_2$ distorted pbps and the planar triangular CO_3 groups share their edges. The interconnection results in isolated $[VO(O_2)_2CO_3]$ units. Interestingly, the $[VO(O_2)_2CO_3]$ groups align parallel to CO_3 in the same direction, which should be extremely beneficial to generating a gigantic macroscopic SHG effect (Fig. 1). [48,49]

Thermogravimetric analysis (TGA) indicates that $Cs_3VO(O_2)_2CO_3$ is thermally stable up to 300 °C (Fig. S3†). Upon further heating under a nitrogen atmosphere, $Cs_3VO(O_2)_2CO_3$ completely decomposes to $Cs_4V_2O_7$, Cs_2O, and CO_2 in two steps in the range of 300–1000 °C. Interestingly, $Cs_3VO(O_2)_2CO_3$ exhibits the highest thermal decomposition temperature (300 °C) among all reported peroxovanadates. In fact, the thermal stability of a series of isostructural compounds, $A_3VO(O_2)_2CO_3$ (A = K, Rb, and Cs), obviously increases as the radii of alkali metal cations increase (see Table 1). A closer structural examination suggests that the thermostability of $A_3VO(O_2)_2CO_3$ seems to be strongly affected by the alkali metal cations' size. Although the $VO_3(O_2)_2$ pbps in $A_3VO(O_2)_2CO_3$ are stabilized by the coordinated bidentate carbonato ligands, the extent of distortion is varied by the different alkali metal cations. Specifically, two unique K^+ cations in $K_3VO(O_2)_2CO_3$ interact with 9 oxide ligands with the K–O contact lengths in the range of 2.6561(18)–3.160(2) Å, and two kinds of Rb^+ cations in $Rb_3VO(O_2)_2CO_3$ contact with 9 and 10 oxides with the Rb–O lengths in the range of 2.769(4)–3.550(4). [41,42] In $Cs_3VO(O_2)_2CO_3$, the interactions between two unique Cs^+ cations and oxide ligands are even longer and reveal Cs–O contact lengths in the range of 2.965(8)–3.687(8) Å.

As seen in Fig. 2, the small ionic size of K^+ in $K_3VO(O_2)_2CO_3$ requires a smaller coordination environment. Substantial interaction between K^+ cations and oxide ligands results in peroxo ligands with shorter O–O distances (1.456 Å) and more strained $VO_3(O_2)_2$ pbps. However, the large Cs^+ cations in $Cs_3VO(O_2)_2CO_3$ with a larger coordination moiety reveal peroxo ligands with
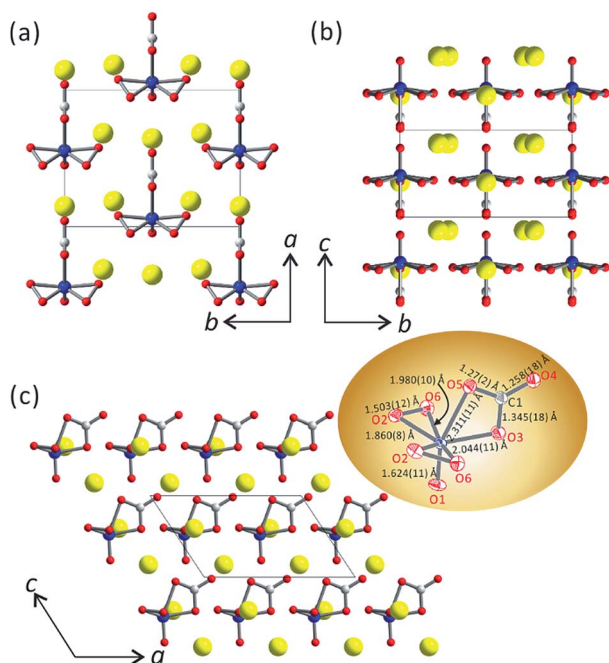

Fig. 1 Ball-and-stick models of $Cs_3VO(O_2)_2CO_3$ in the (a) *ab* plane, (b) *bc* plane, and (c) *ac* plane (yellow, Cs; blue, V; gray, C; and red, O). The $[VO(O_2)_2CO_3]$ units align parallel to CO_3 groups and orient in the same direction.

Table 1 Thermal and optical properties of $A_3VO(O_2)_2CO_3$ (A = K, Rb, and Cs)

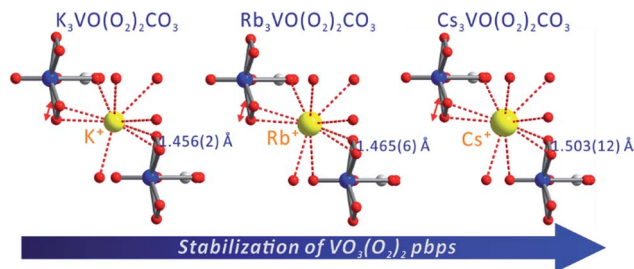| Compound	dec. T (°C)	E_g (eV)	d(O–O) in $(O_2)^{2-}$ (Å)
$K_3VO(O_2)_2CO_3$	230	2.57	1.456
$Rb_3VO(O_2)_2CO_3$	250	2.68	1.465
$Cs_3VO(O_2)_2CO_3$	300	2.81	1.503

Fig. 2 Ball-and-stick models revealing the effect of the size of alkali metal cations on the stability of VO$_3$(O$_2$)$_2$ pbps in A$_3$VO(O$_2$)$_2$CO$_3$. While the shorter O−O distances in peroxo ligands due to the smaller coordination environment of K$^+$ result in more strained VO$_3$(O$_2$)$_2$ pbps, the longer O−O distances in peroxo ligands attributed to the large Cs$^+$ generate less strained stable VO$_3$(O$_2$)$_2$ pbps.

Fig. 4 Phase-matching curve for Cs$_3$VO(O$_2$)$_2$CO$_3$. The inset reveals oscilloscope traces showing the SHG intensity for A$_3$VO(O$_2$)$_2$CO$_3$ (A = K, Rb, and Cs). The SHG intensities for KDP, KTP, and KSrCO$_3$F are also plotted for comparison.

longer O–O distances (1.503 Å) and less strained and more stable VO$_3$(O$_2$)$_2$ pbps. Accordingly, the thermal stability of A$_3$VO(O$_2$)$_2$CO$_3$ (A = K, Rb, and Cs) increases in the K < Rb < Cs order attributable to the stability of the corresponding pbps.

The infrared (IR) spectrum of Cs$_3$VO(O$_2$)$_2$CO$_3$ revealed intense broad bands at 1370 and 1590 cm^{-1} attributed to the C–O stretching vibrations in the triangular CO$_3$ groups and bands at 850 and 700–640 cm^{-1} due to the nonplanar bending vibrations of CO$_3$ plane triangles (Fig. S4†). Bands observed at 1020 and 920 cm^{-1} were assigned to the characteristic absorption of ν_{V-O}. The assignments are consistent with other metal carbonatoperoxovanadates.[50]

The UV-vis diffuse reflectance spectrum of Cs$_3$VO(O$_2$)$_2$CO$_3$ was collected, and the absorption (K/S) data were calculated by the Kubelka–Munk function (Fig. 3).[51,52] The optical band gap for Cs$_3$VO(O$_2$)$_2$CO$_3$ is 2.81 eV, indicating that the material is a wide band-gap semiconductor. The transmittance spectrum (Fig. S5†) and the UV absorption spectrum show that there is no absorption from 0.35 to 2.5 μm, suggesting that Cs$_3$VO(O$_2$)$_2$CO$_3$ has wide transparent regions ranging from near-UV to mid-IR.

Also in A$_3$VO(O$_2$)$_2$CO$_3$ (A = K, Rb, and Cs), the experimental band gaps increase with increasing the radius of cations (Table 1 and Fig. S7†). The observed band gaps are closely related to the distortion of VO$_3$(O$_2$)$_2$ pbps because the main contribution of the lowest part of the conduction band is d- and p-orbitals of V and O atoms, respectively (Fig. S9†). As we described earlier, the highly distorted VO$_3$(O$_2$)$_2$ pbps in contact with the smaller coordination environment of K$^+$ reveal a relatively smaller band gap, whereas the less strained VO$_3$(O$_2$)$_2$ pbps interacting with the large Cs$^+$ exhibit a larger band gap. In fact, the experimental results are in good agreement with the calculated band gaps (Fig. S10†).

The SHG responses of Cs$_3$VO(O$_2$)$_2$CO$_3$ were measured on sieved ground crystals (Fig. 4). The SHG signals increase gradually with the increasing particle size of samples at the beginning and then tend to remain constant from 155 μm, indicating that Cs$_3$VO(O$_2$)$_2$CO$_3$ is type I phase-matchable. The title compound exhibits an extremely strong SHG response of ca. 23.0 times that of KDP, almost 7 times that of KSrCO$_3$F, which is the largest among those of all the NLO carbonates, including CsPbCO$_3$F (13 × KDP),[32] RbCdCO$_3$F (9 × KDP),[53] and K$_4$Eu$_2$(CO$_3$)$_3$F$_4$ (8 × KDP),[54] reported to date. In addition, as seen in Fig. 4 and Table 2, the SHG efficiencies of the isostructural compounds A$_3$VO(O$_2$)$_2$CO$_3$ (A = K, Rb, and Cs)

Fig. 3 UV-vis-NIR transmittance spectrum of Cs$_3$VO(O$_2$)$_2$CO$_3$. The inset shows an optical diffuse reflectance spectrum of Cs$_3$VO(O$_2$)$_2$CO$_3$.

Table 2 NLO Effects of A$_3$VO(O$_2$)$_2$CO$_3$ (A = K, Rb, and Cs) and KSrCO$_3$F

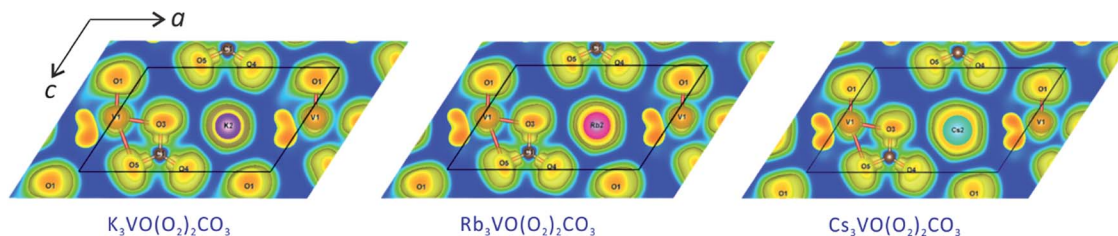| Compound	SHG (×KDP)	Structural criterion, C	Density of [CO$_3$]$^{2-}$, (n/V) (Å)	(n/V) × C (Å)
K$_3$VO(O$_2$)$_2$CO$_3$	20.0	1.00	0.0051	0.0051
Rb$_3$VO(O$_2$)$_2$CO$_3$	21.0	1.00	0.0046	0.0046
Cs$_3$VO(O$_2$)$_2$CO$_3$	23.0	1.00	0.0041	0.0041
KSrCO$_3$F	3.3	1.00	0.0089	0.0089

Fig. 5 Three sliced-planes of electron localization function (ELF) of $A_3VO(O_2)_2CO_3$ (A = K, Rb, and Cs) in the crystallographic ac-plane. All diagrams are depicted as filled contour maps. The color scheme ranges from blue to red ($0-0.7$ e$^-$ per Å^3), and values higher than 0.5 represent the area exceeding the free-electron ELF value. The unit cell is outlined in black.

increase with increasing the size of alkali metal cations. The anionic group theory indicates that the values of intra-atomic dipole transitions in anionic groups are larger than those of the transitions occurring from the cations to the anionic groups which are off-site transitions.[43,55] Thus, the NLO coefficients of $Cs_3VO(O_2)_2CO_3$ mainly originate from CO_3 plane triangle groups. The major determinants for the NLO coefficients of the title compound are two: the structural criterion (C) and the density of anionic groups (n/V) ($[CO_3]^{2-}$ in this case). A high C value (100%) results from the optimal arrangement of CO_3 plane triangle groups in $A_3VO(O_2)_2CO_3$ (A = K, Rb, and Cs) as those in $KSrCO_3F$,[31] with all CO_3 groups arranging in parallel and orienting in the same direction. Thus, the density of CO_3 groups determines the macroscopic NLO coefficients of these four carbonate NLO materials.

Interestingly, $Cs_3VO(O_2)_2CO_3$ exhibits an unexpectedly strong SHG response (7.0 × $KSrCO_3F$), although the density of aligned CO_3 groups in $Cs_3VO(O_2)_2CO_3$ is less than half compared to that of $KSrCO_3F$ (Table 2). Therefore, we believe that there are some other factors that affect the striking SHG intensity of $Cs_3VO(O_2)_2CO_3$ in addition to the anionic group theory. The distorted environment of $VO_3(O_2)_2$ pbps in $Cs_3VO(O_2)_2CO_3$ should be an important contribution factor, which was confirmed by the calculated dipole moment value of 12.4 D (debyes) with a net moment of *ca.* 24.8 D for a unit cell along the c-direction. In addition, polarizability of Cs^+ cations is another crucial factor influencing the SHG response. Comparing the three isostructural compounds, $A_3VO(O_2)_2CO_3$ (A = K, Rb, and Cs), we found that the SHG responses obviously increase with increasing the radii of cations. The electron localization function (ELF) diagrams of $A_3VO(O_2)_2CO_3$ (A = K, Rb, and Cs) are displayed in the crystallographic ac-plane in Fig. 5. It is clear that O1, O3, O4, and O5 atoms forming the $VO_3(O_2)_2$ pbps reveal strongly distorted ELF values. In particular, the distortion of O3 forming the trigonal $(CO_3)^{2-}$ group toward nearby cations increases as the polarizability of cations increases from K to Rb and to Cs. Therefore, the increasing trend of SHG response of these compounds should be attributed to the increasing polarizability of cations as well as the interatomic interactions with neighboring O atoms.

The calculated linear optical results show that the refractive index dispersion curves display strong anisotropy and follow the order of $n_z > n_y \approx n_x$ with a moderate birefringence (Δn) (0.105@1064 nm), which is in favor of phase-matching during the SHG process (Fig. S11†). On the basis of the space group and

Kleinman symmetry,[56,57] there exist six non-zero independent SHG coefficient tensors for $Cs_3VO(O_2)_2CO_3$ (d_{11}, d_{12}, d_{13}, d_{15}, d_{24}, and d_{33}). The absolute value of d_{13}, the highest tensor, in the static limit is calculated to be 8.7 pm V^{-1} at a wavelength of 1064 nm, which agrees well with our experimental value (Fig. S12†).

Conclusions

A novel superb NLO carbonatoperoxovanadate material, $Cs_3VO(O_2)_2CO_3$, has been successfully designed and synthesized by introducing highly polarizable cations and inorganic polydentate carbonato ligands into asymmetric peroxovanadates. $Cs_3VO(O_2)_2CO_3$ exhibits a thermal decomposition temperature of 300 °C, which is the highest among those of all the reported peroxovanadates. $Cs_3VO(O_2)_2CO_3$ also reveals an extremely strong SHG intensity of 23.0 × KDP, which is the largest value ever observed in the current carbonate NLO materials. Detailed structural investigations along with theoretical calculations confirmed that the extremely large SHG intensity originates from the cooperation of the NCS chromophores composed of CO_3 planar triangle groups with delocalized π orbitals, O_2^{2-} groups with distorted localized π orbitals, highly polarizable Cs^+ cations, and SOJT distortive V^{5+} cation polyhedra. We found that careful tuning of the polarizability and the size of alkali metal cations is extremely important to design novel NLO materials with excellent performance.

Conflicts of interest

There are no conflicts to declare.

Acknowledgements

Notes and references

1 P. S. Halasyamani and K. R. Poeppelmeier, *Chem. Mater.*, 1998, **10**, 2753–2769.

2 H. W. Yu, H. P. Wu, S. L. Pan, Z. H. Yang, X. L. Hou, X. Su, Q. Jing, K. R. Poeppelmeier and J. M. Rondinelli, *J. Am. Chem. Soc.*, 2014, **136**, 1264–1267.

3 K. M. Ok, *Acc. Chem. Res.*, 2016, **49**, 2774–2785.

4 T. T. Tran, J. Young, J. M. Rondinelli and P. S. Halasyamani, *J. Am. Chem. Soc.*, 2016, **139**, 1285–1295.

5 G. Zou, C. Lin, H. Jo, G. Nam, T. S. You and K. M. Ok, *Angew. Chem., Int. Ed.*, 2016, **55**, 12078–12082.

6 L. Huang, Q. Wang, C. Lin, G. Zou, D. Gao, J. Bi and N. Ye, *J. Alloys Compd.*, 2017, **724**, 1057–1063.

7 T. T. Tran, N. Z. Koocher, J. M. Rondinelli and P. S. Halasyamani, *Angew. Chem., Int. Ed.*, 2017, **56**, 2969–2973.

8 G. Shi, Y. Wang, F. Zhang, B. Zhang, Z. Yang, X. Hou, S. Pan and K. R. Poeppelmeier, *J. Am. Chem. Soc.*, 2017, **139**, 10645–10648.

9 X. Wang, Y. Wang, B. Zhang, F. Zhang, Z. Yang and S. Pan, *Angew. Chem., Int. Ed.*, 2017, **56**, 14119–14123.

10 B. Zhang, G. Shi, Z. Yang, F. Zhang and S. Pan, *Angew. Chem., Int. Ed.*, 2017, **56**, 3916–3919.

11 X. Dong, L. Huang, Q. Liu, H. Zeng, Z. Lin, D. Xu and G. Zou, *Chem. Commun.*, 2018, **54**, 5792–5795.

12 M. Mutailipu, M. Zhang, B. Zhang, L. Wang, Z. Yang, X. Zhou and S. Pan, *Angew. Chem., Int. Ed.*, 2018, **57**, 6095–6099.

13 Q. Wang, F. He, L. Huang, D. Gao, J. Bi and G. Zou, *Cryst. Growth Des.*, 2018, **18**, 3644–3653.

14 Q. Wang, C. Lin, G. Zou, M. Liu, D. Gao, J. Bi and L. Huang, *J. Alloys Compd.*, 2018, **735**, 677–683.

15 Y. Wang, B. Zhang, Z. Yang and S. Pan, *Angew. Chem., Int. Ed.*, 2018, **57**, 2150–2154.

16 L. Kang, S. Luo, H. Huang, N. Ye, Z. Lin, J. Qin and C. Chen, *J. Phys. Chem. C*, 2013, **117**, 25684–25692.

17 S. Zhao, L. Kang, Y. Shen, X. Wang, M. A. Asghar, Z. Lin, Y. Xu, S. Zeng, M. Hong and J. Luo, *J. Am. Chem. Soc.*, 2016, **138**, 2961–2964.

18 M. Luo, F. Liang, Y. Song, D. Zhao, F. Xu, N. Ye and Z. Lin, *J. Am. Chem. Soc.*, 2018, **140**, 3884–3887.

19 M. Luo, F. Liang, Y. Song, D. Zhao, N. Ye and Z. Lin, *J. Am. Chem. Soc.*, 2018, **140**, 6814–6817.

20 G. A. Samara, *Ferroelectrics*, 1973, **5**, 25–37.

21 F. C. Zumsteg, J. D. Bierlein and T. E. Gier, *J. Appl. Phys.*, 1976, **47**, 4980–4985.

22 G. D. Boyd, R. C. Miller, K. Nassau, W. L. Bond and A. Savage, *Appl. Phys. Lett.*, 1964, **5**, 234–236.

23 C. Chen, Y. Wu, A. Jiang, B. Wu, G. You, R. Li and S. Lin, *J. Opt. Soc. Am. B*, 1989, **6**, 616–621.

24 C. T. Chen, B. C. Wu and A. D. Jiang, *Sci. Sin., Ser. B*, 1985, **28**, 235–243.

25 A. Harasaki and K. Kato, *Jpn. J. Appl. Phys.*, 1997, **36**, 700–703.

26 H. Huang, J. Yao, Z. Lin, X. Wang, R. He, W. Yao, N. Zhai and C. Chen, *Chem. Mater.*, 2011, **23**, 5457–5463.

27 S. C. Wang and N. Ye, *J. Am. Chem. Soc.*, 2011, **133**, 11458–11461.

28 H.-S. Ra, K. M. Ok and P. S. Halasyamani, *J. Am. Chem. Soc.*, 2003, **125**, 7764–7765.

29 Y.-Z. Huang, L.-M. Wu, X.-T. Wu, L.-H. Li, L. Chen and Y.-F. Zhang, *J. Am. Chem. Soc.*, 2010, **132**, 12788–12789.

30 W.-L. Zhang, W.-D. Cheng, H. Zhang, L. Geng, C.-S. Lin and Z.-Z. He, *J. Am. Chem. Soc.*, 2010, **132**, 1508–1509.

31 G. H. Zou, N. Ye, L. Huang and X. S. Lin, *J. Am. Chem. Soc.*, 2011, **133**, 20001–20007.

32 G. H. Zou, L. Huang, N. Ye, C. S. Lin, W. D. Cheng and H. Huang, *J. Am. Chem. Soc.*, 2013, **135**, 18560–18566.

33 S. Zhao, P. Gong, L. Bai, X. Xu, S. Zhang, Z. Sun, Z. Lin, M. Hong, C. Chen and J. Luo, *Nat. Commun.*, 2014, **5**, 1–7.

34 L. Huang, G. H. Zou, H. Q. Cai, S. C. Wang, C. S. Lin and N. Ye, *J. Mater. Chem. C*, 2015, **3**, 5268–5274.

35 S. Zhao, P. Gong, S. Luo, S. Liu, L. Li, M. A. Asghar, T. Khan, M. Hong, Z. Lin and J. Luo, *J. Am. Chem. Soc.*, 2015, **137**, 2207–2210.

36 M. Xia, X. Jiang, Z. Lin and R. Li, *J. Am. Chem. Soc.*, 2016, **138**, 14190–14193.

37 S. Zhao, Y. Yang, Y. Shen, B. Zhao, L. Li, C. Ji, Z. Wu, D. Yuan, Z. Lin, M. Hong and J. Luo, *Angew. Chem., Int. Ed.*, 2016, **56**, 540–544.

38 F. F. Mao, C. L. Hu, X. Xu, D. Yan, B. P. Yang and J. G. Mao, *Angew. Chem., Int. Ed.*, 2017, **56**, 2151–2155.

39 Y. Shen, S. Zhao and J. Luo, *Coord. Chem. Rev.*, 2018, **366**, 1–28.

40 M. L. Liang, Y. X. Ma, C. L. Hu, F. Kong and J.-G. Mao, *Dalton Trans.*, 2018, **47**, 1513–1519.

41 Y. Song, M. Luo, F. Liang, N. Ye and Z. Lin, *Chem. Commun.*, 2018, **54**, 1445–1448.

42 G. Zou, H. Jo, S. J. Lim, T. S. You and K. M. Ok, *Angew. Chem., Int. Ed.*, 2018, **57**, 8619–8622.

43 N. Ye, Q. Chen, B. Wu and C. Chen, *J. Appl. Phys.*, 1998, **84**, 555–558.

44 L. Li, Y. Wang, B. H. Lei, S. Han, Z. Yang, K. R. Poeppelmeier and S. Pan, *J. Am. Chem. Soc.*, 2016, **138**, 9101.

45 Y. Shen, Y. Yang, S. Zhao, B. Zhao, Z. Lin, C. Ji, L. Li, P. Fu, M. Hong and J. Luo, *Chem. Mater.*, 2016, **28**, 7110–7116.

46 X. Cheng, M. H. Whangbo, G. C. Guo, M. Hong and S. Deng, *Angew. Chem., Int. Ed.*, 2018, **57**, 3933–3937.

47 H. P. Wu, H. W. Yu, Z. H. Yang, X. L. Hou, X. Su, S. L. Pan, K. R. Poeppelmeier and J. M. Rondinelli, *J. Am. Chem. Soc.*, 2013, **135**, 4215–4218.

48 P. A. Maggard, T. S. Nault, C. L. Stern and K. R. Poeppelmeier, *J. Solid State Chem.*, 2003, **175**, 27–33.

49 P. Yu, L.-J. Zhou and L. Chen, *J. Am. Chem. Soc.*, 2012, **134**, 2227–2235.

50 A. Butler, M. J. Clague and G. E. Meister, *Chem. Rev.*, 1994, **94**, 625–638.

51 P. Kubelka, *Z. Tech. Phys.*, 1931, **12**, 593–603.

52 J. Tauc, *Mater. Res. Bull.*, 1970, **5**, 721–729.

53 G. Zou, G. Nam, H. G. Kim, H. Jo, T.-S. You and K. M. Ok, *RSC Adv.*, 2015, **5**, 84754–84761.

54 J. D. Grice, V. Maisonneuve and M. Leblanc, *Chem. Rev.*, 2007, **107**, 114–132.

55 C. Chen, Y. Wu and R. Li, *Int. Rev. Phys. Chem.*, 1989, **8**, 65–91.

56 J. F. Nye, *Physical Properties of Crystals*, Oxford University Press, Oxford, UK, 1957.

57 D. A. Kleinman, *Phys. Rev.*, 1962, **126**, 1977–1979.